Electronic supplementary information (ESI) for

Meldrum's acid mediated ketene chemistry in formation of ester bonds for synthesis of vitrimers with high glass transition temperatures

*Du-Yuan Hung and Ying-Ling Liu**

Department of Chemical Engineering, National Tsing Hua University, No. 101, Sec. 2, Kuang-Fu Road, Hsinchu 300044, Taiwan.

* Corresponding author, E-mail: liuyl@mx.nthu.edu.tw

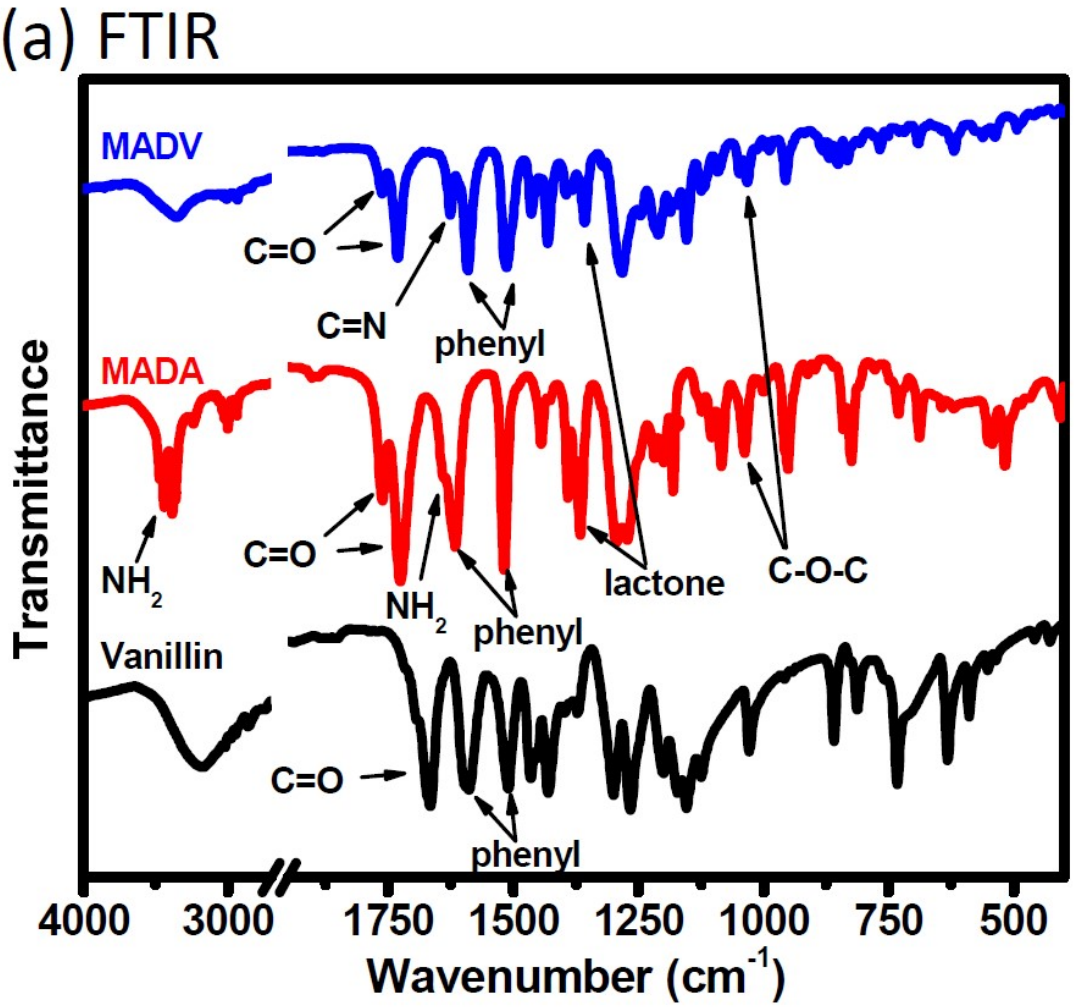

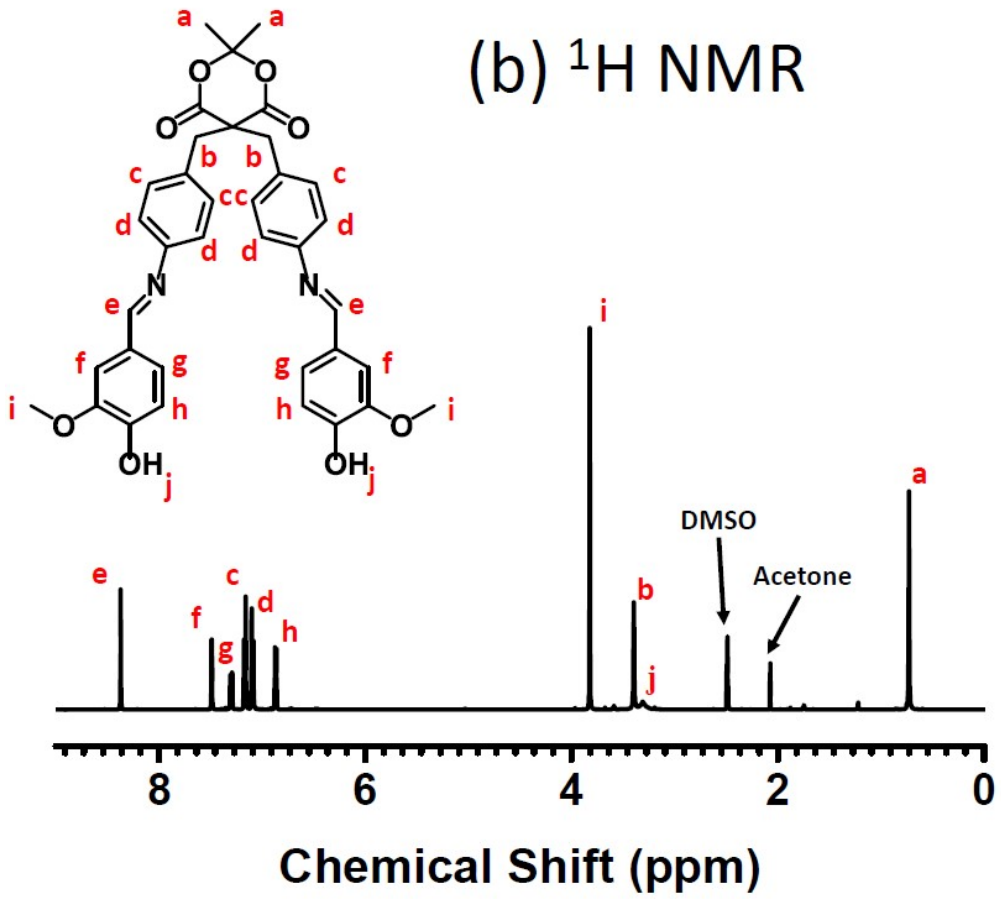
(b) 1H NMR
DMSO
Acetone
8
6
4
2
0
Chemical Shift (ppm)

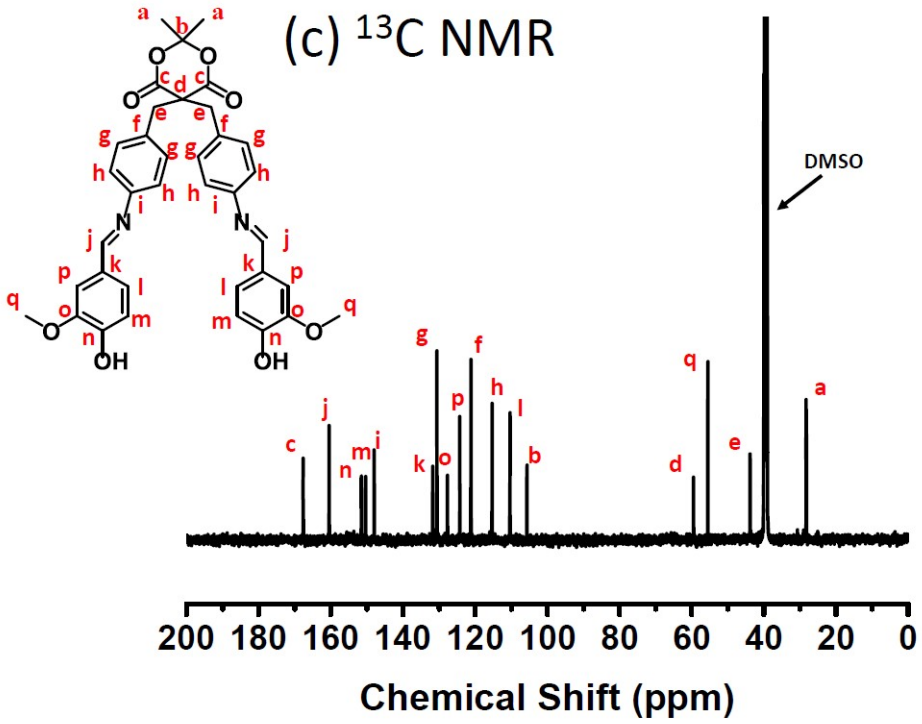
(c) 13C NMR
DMSO
200 180 160 140 120 100 80 60 40 20 0
Chemical Shift (ppm)

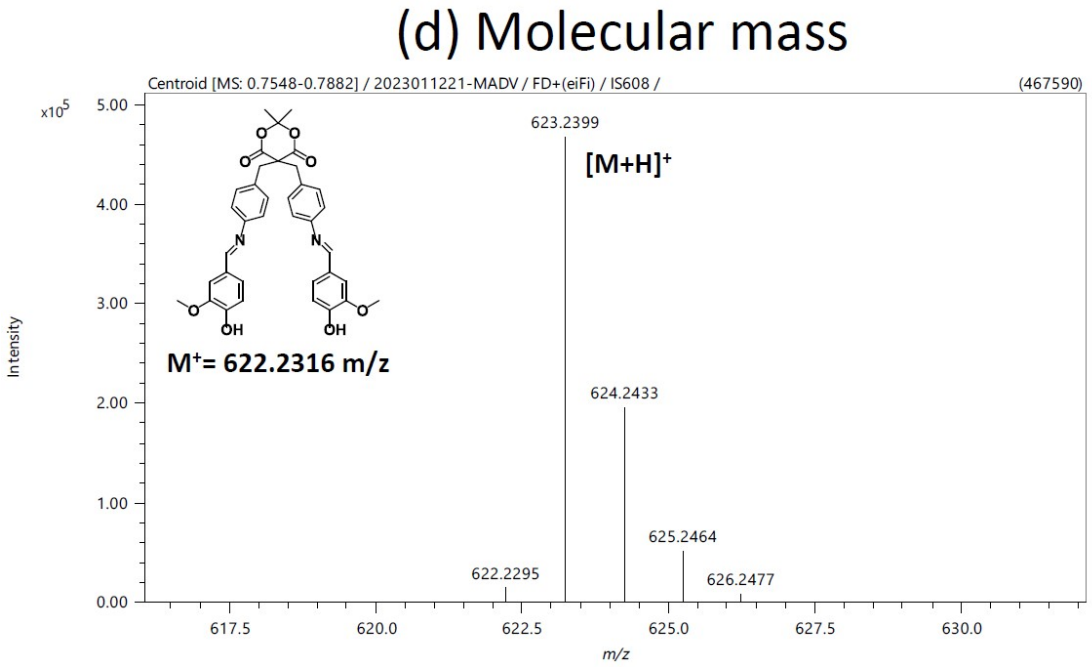

Figure S1. Spectral characterization of MADV with (a) FTIR, (b) ^{1}H NMR, (c) ^{13}C NMR, and (d) molecular mass instruments. It is noted that the acetone signals could be from the residual solvent employed in the synthesis and purification processes.

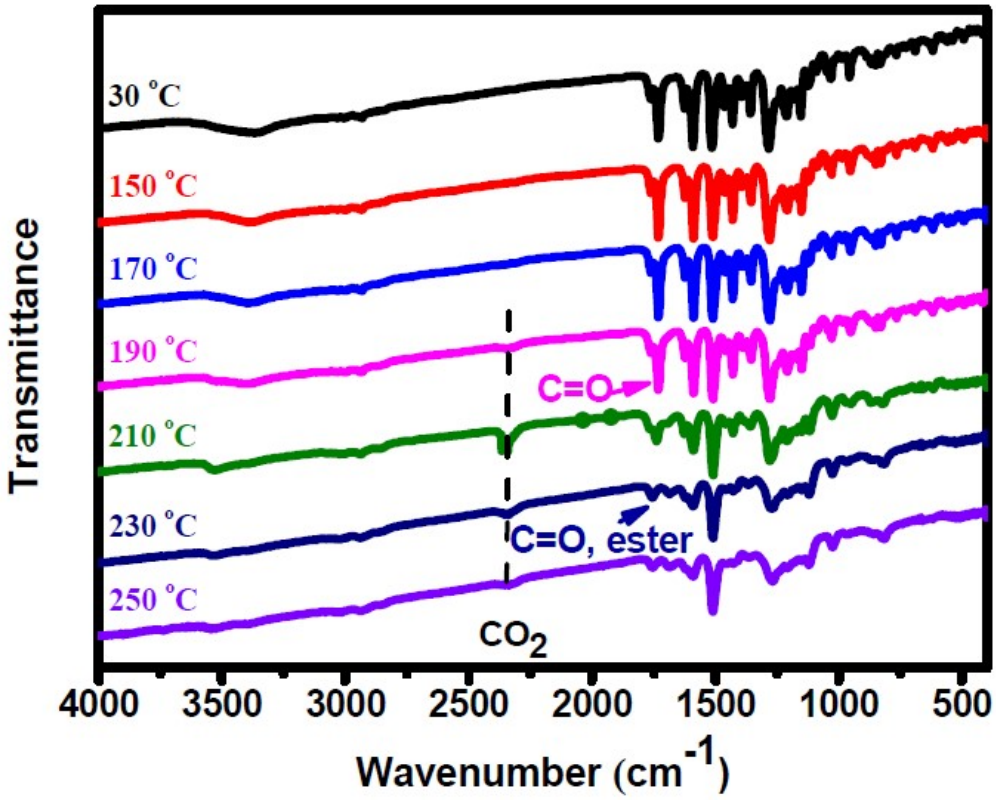

Figure S2. FTIR spectra of MADV recorded at different temperatures for tracing the occurrence of MA thermolysis reaction.

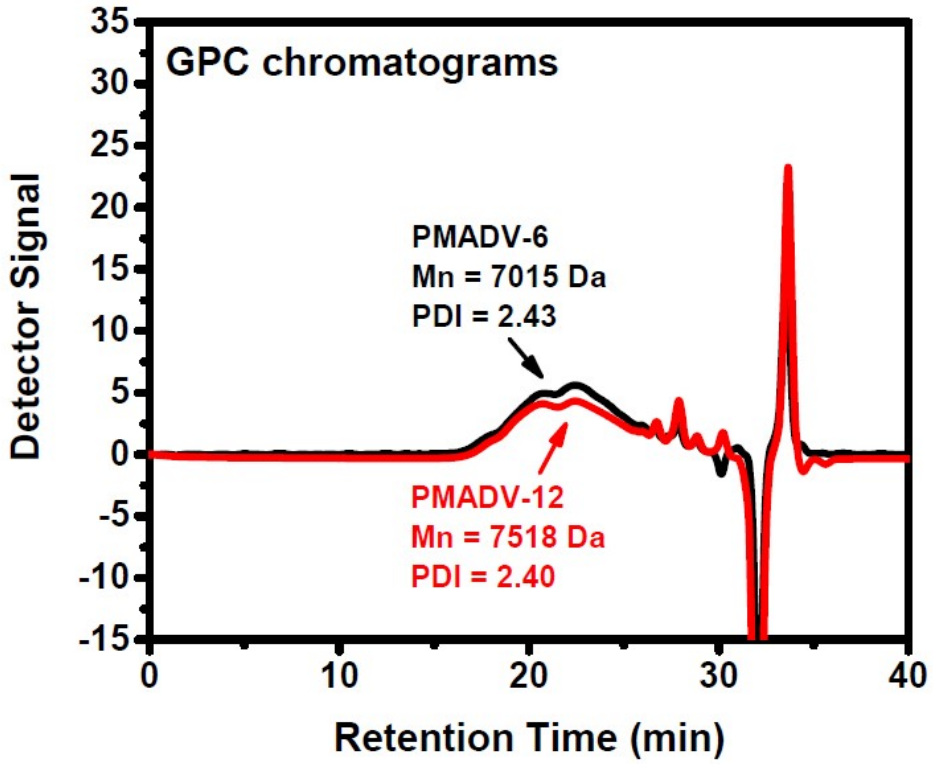

Figure S3. GPC chromatograms of PMADV-6 and PMADV-12 for determination their molecular weights.

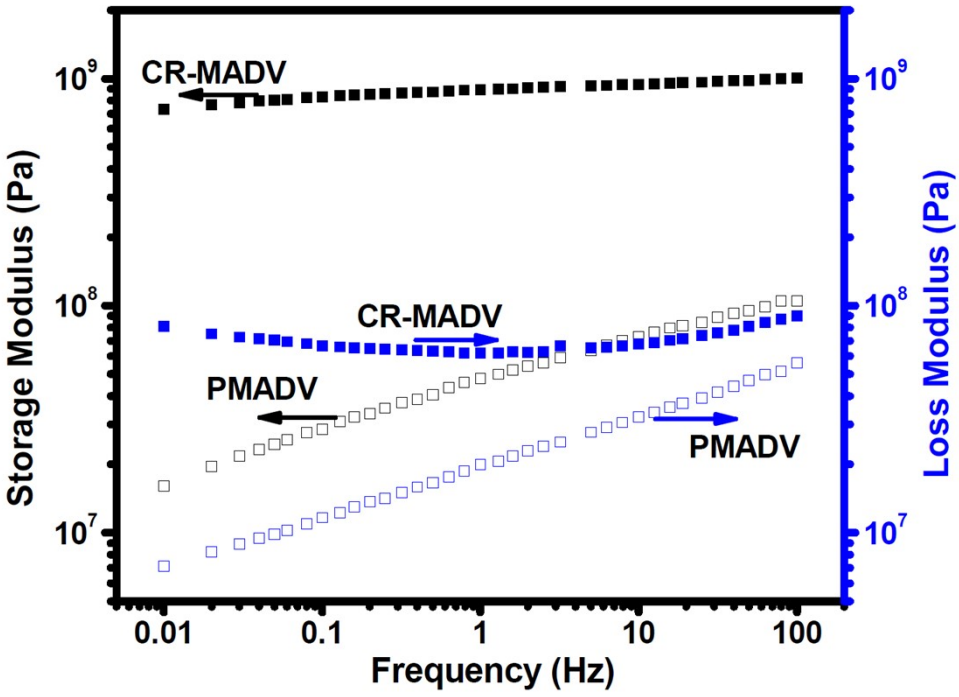

Figure S4. Storage modulus and loss modulus of PMADV and CR-MADV recorded at 150 ^{o}C and various frequencies.

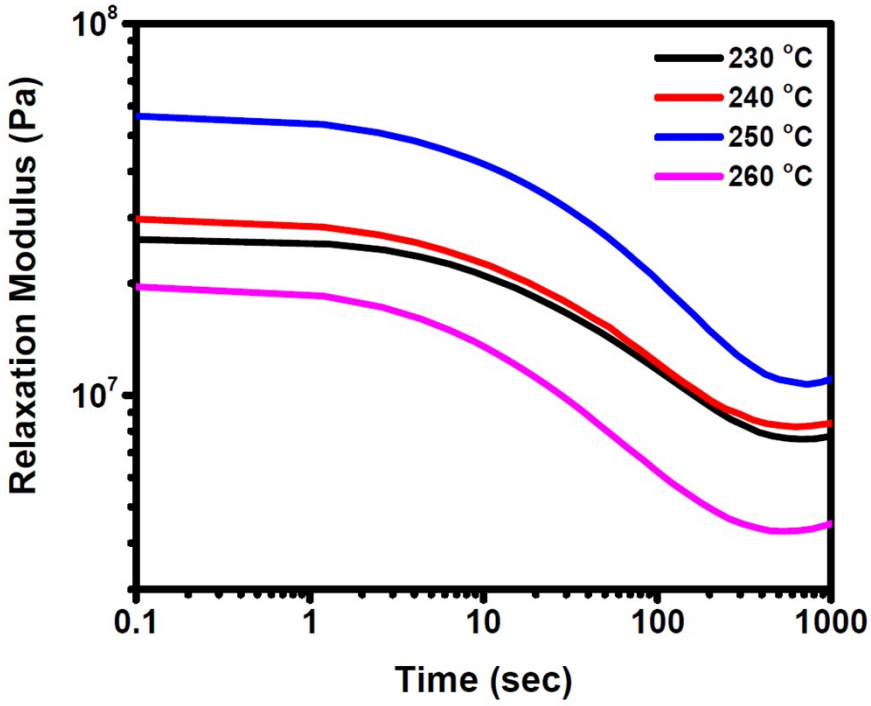

Figure S5. Stress relaxation curves of CR-MADV recorded at various temperatures.

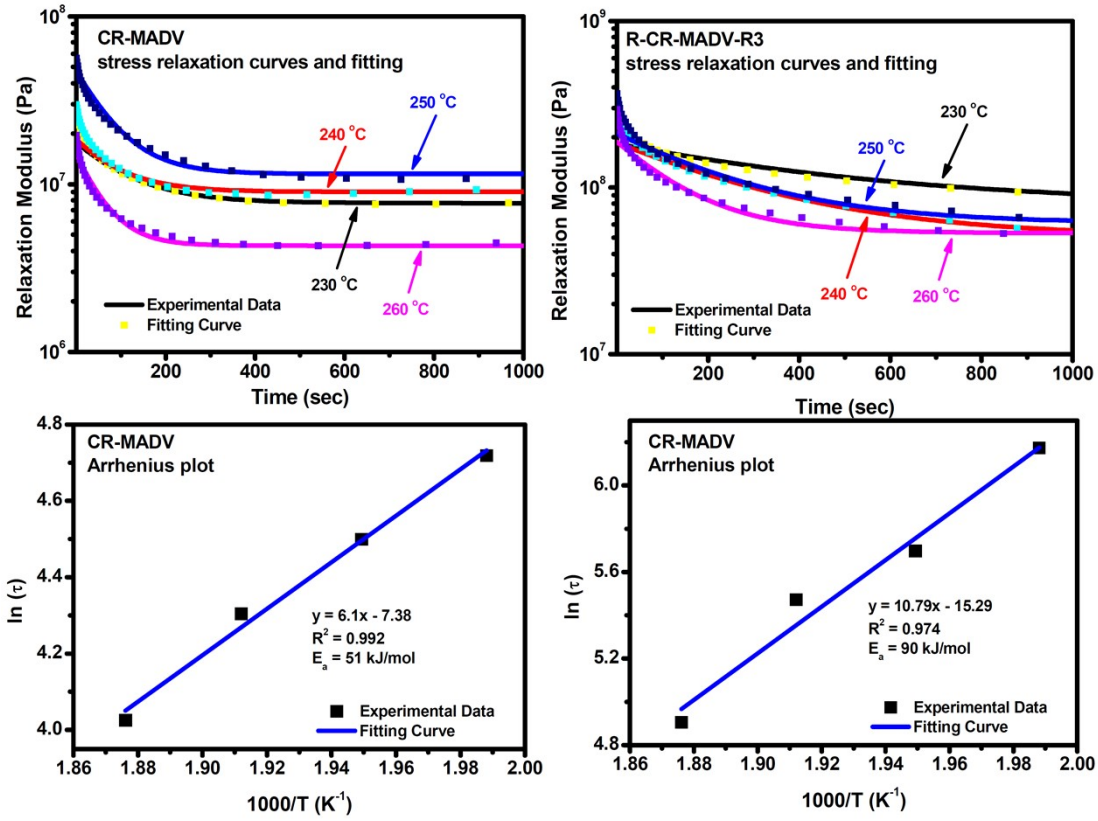

Figure S6. Stress relaxation curves with curve fitting (upper) and Arrhenius plots (lower) of CR-MADV and R-CR-MADV-3.

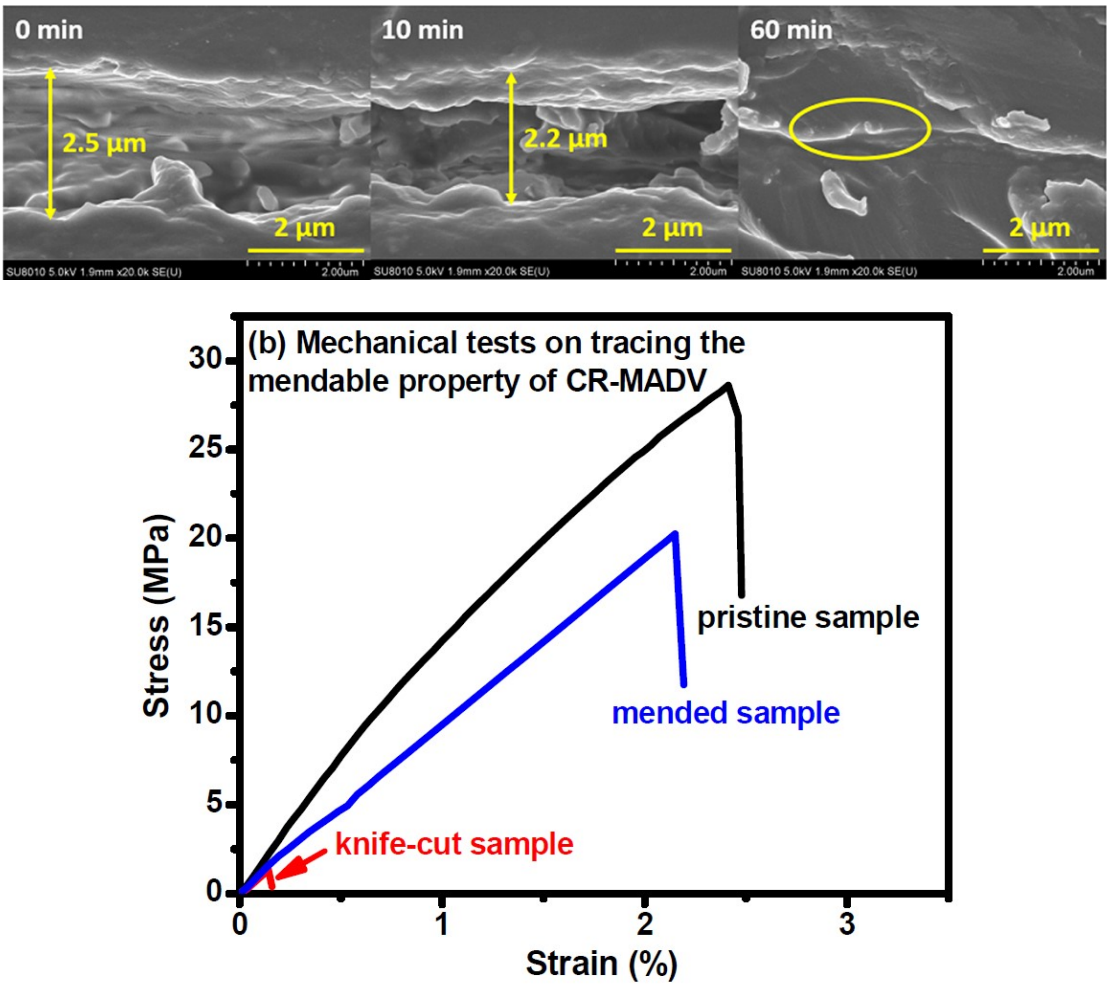

Figure S7. (a) SEM micrographs and (b) stress-strain curves tracing the mendable tests of CR-MADV at 230 °C under an applied pressure of about of about 34,000 N m^{-2}. The SEM pictures in relatively high magnification exhibiting the mended cutprint of the sample.

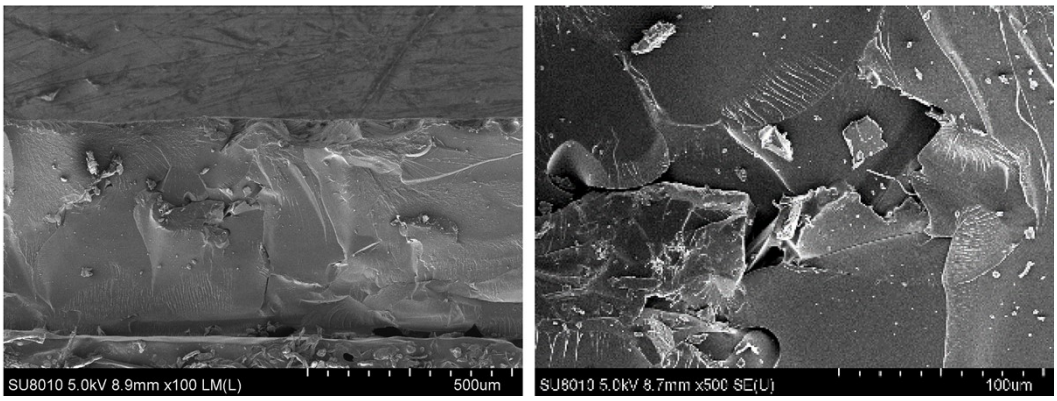

Figure S8. SEM microgrphas of the recycled sample of CR-MADV obtained from thermal press at 200 °C and 5 MPa for 1 h.

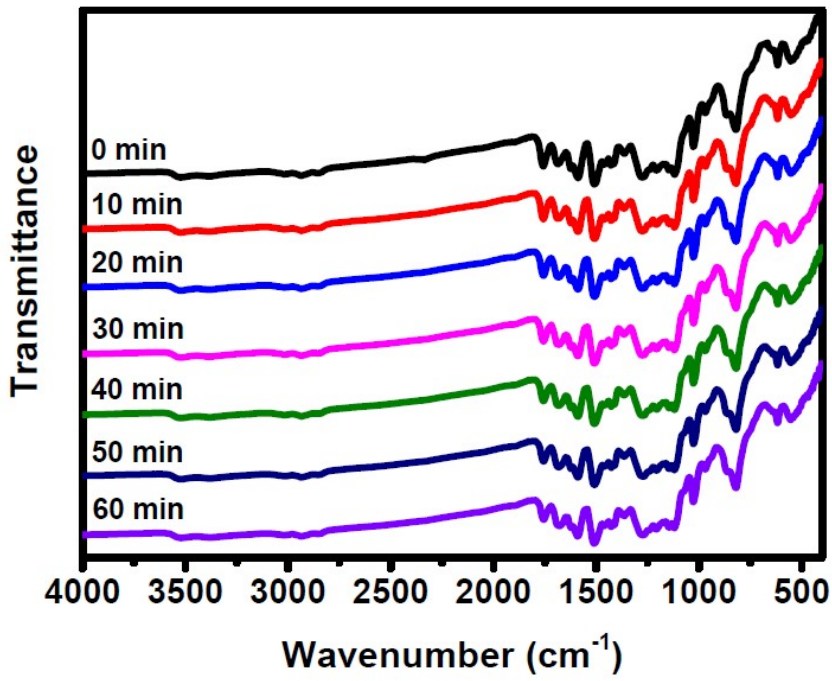

Figure S9. FTIR measurements on CR-MADV isothermally at 230 °C, indicating no obvious changes in the chemical structure being observed in the duration of reprocessing.

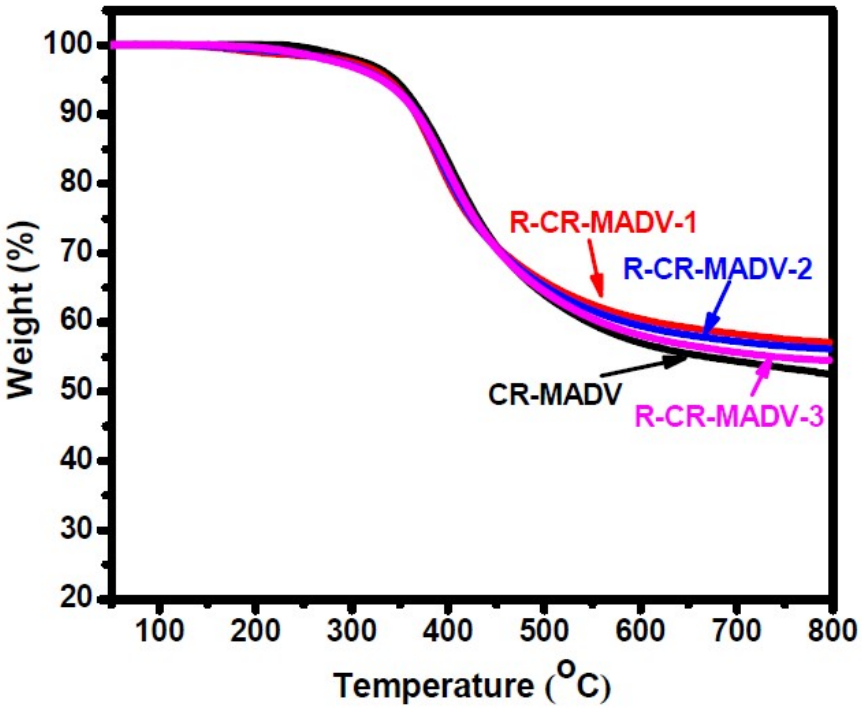

Figure S10. TGA thermograms of CR-MADV and the thermally recycled samples (R-CR-MADV), indicating no obvious changes in thermal stability of CR-MADV after being thermally recycled.

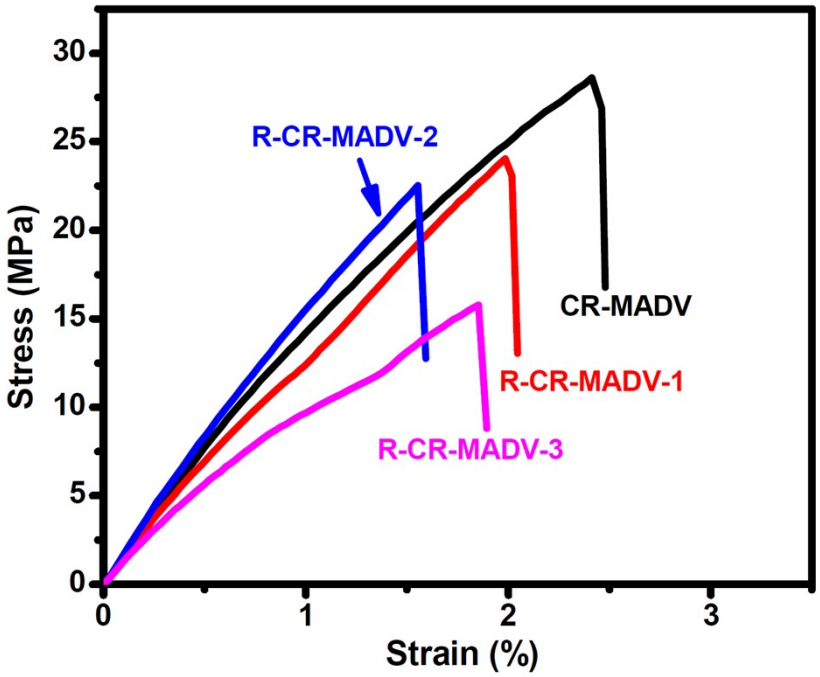

Figure S11. Stress-strain curves of CR-MADV and the thermally recycled samples (R-CR-MADV.

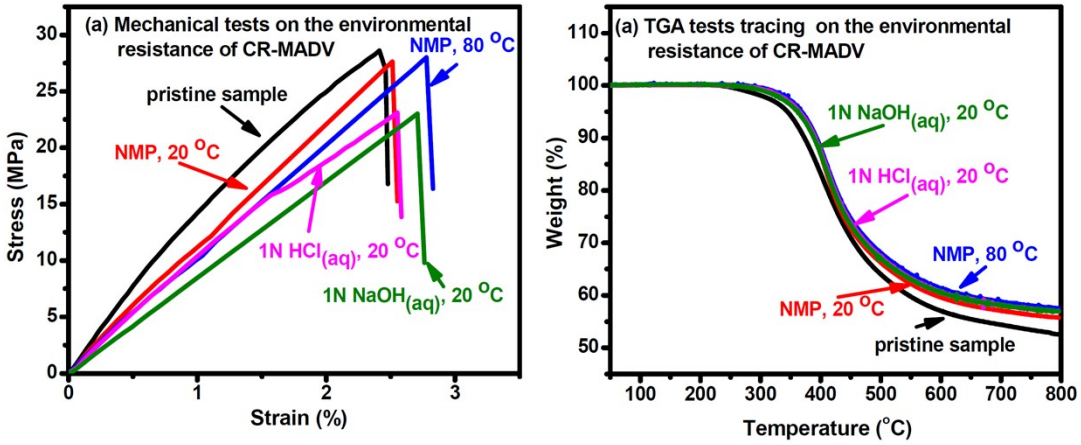

Figure S12. *(a)* Stress-strain curves and (b) TGA thermograms of pristine, solvent-(NMP), acid-, and base-treated CR-MADV samples.

Table S1. Mechanical properties of CR-MADV and the thermally recycled samples.

Sample	Young's modulus (GPa)	Tensile strength (MPa)	Elongation at break (%)	Recycling efficiency (%)
CR-MADV	1.58	28.6	2.4	--
R-CR-MADV-1	1.48	24.0	2.0	84
R-CR-MADV-2	1.78	22.5	1.5	94
R-CR-MADV-3	1.22	15.8	1.8	70

Table S2. Gel fractions (%) of CR-MADV and the thermally recycled samples.

Sample	Gel fraction (wt%)		
	NMP	1 N $HCl_{(aq)}$	1 N $NaOH_{(aq)}$
CR-MADV	99.1	97	96.8
R-CR-MADV-1	99.4	96.8	98.4
R-CR-MADV-2	98.9	96.2	98.4
R-CR-MADV-3	97.8	95.2	98.5